CHARACTERIZATION OF THE MOBILITIES OF SELECTED ACTINIDES AND FISSION/ACTIVATION PRODUCTS IN LABORATORY COLUMNS CONTAINING SUBSURFACE MATERIAL FROM THE SNAKE RIVER PLAIN

FUEL CYCLE AND MANAGEMENT

KEYWORDS: *radionuclide mobility, subsurface media, laboratory column studies*

ROBERT A. FJELD,* TIMOTHY A. DeVOL, RUSSELL W. GOFF,†
MATTHEW D. BLEVINS,‡ DAVID D. BROWN,‡ STEVEN M. INCE,§
and ALAN W. ELZERMAN *Clemson University*
Department of Environmental Engineering and Science
342 Computer Court, Anderson, South Carolina 29625

MEREDITH E. NEWMAN|| *Idaho National Engineering and Environmental Laboratory*
Lockheed Martin Idaho Technologies Corporation, Idaho Falls, Idaho 83415

Received April 27, 1999
Accepted for Publication November 7, 2000

Laboratory column tests were performed to characterize the mobilities of ^{60}Co, ^{90}Sr, ^{137}Cs, ^{233}U, ^{239}Pu, and ^{241}Am in a basalt sample and a composite of sedimentary interbed from the Snake River Plain at the Idaho National Engineering and Environmental Laboratory. The radionuclides were spiked into a synthetic groundwater (pH 8, ionic strength = 0.004 M) and introduced into the columns (D = 2.6 cm, L = 15.2 cm) as finite steps with a width of 1 pore volume followed by unspiked synthetic groundwater. The effluent concentrations were measured continuously for up to 200 pore volumes. Hydrogen-3 was used as a nonreactive tracer in all of the experiments to monitor for channeling. In the basalt sample, the behavior of ^{90}Sr, ^{137}Cs, and ^{233}U was quite different from that of ^{60}Co, ^{239}Pu, and ^{241}Am. The column effluent curves for the former were characterized by single peaks containing, within the limits of experimental uncertainty, all of the activity in the spike. The mobilities were ordered as follows: ^{233}U ($\bar{R} = 5.6$) > ^{90}Sr ($\bar{R} = 29$) > ^{137}Cs ($\bar{R} = 79$). The curves for the other radionuclides were characterized by two or three fractions, each having a distinctly different mobility. Cobalt-60 had high- ($\bar{R} = < 3$), intermediate- ($\bar{R} = 34$), and low- ($R > 200$) mobility fractions. Although a majority of the ^{239}Pu and ^{241}Am had low mobility ($R > 200$), there were high-mobility ($R < 3$) fractions of each (17 to 29% for ^{239}Pu and 7 to 12% for ^{241}Am). In sedimentary interbed, mobilities were generally much lower than in basalt. Uranium-233 was the only radionuclide with 100% recovery within 200 displaced pore volumes, and it had a retardation factor of 30. However, high-mobility fractions were observed for ^{60}Co (1 to 4%) and ^{239}Pu (1.1 to 2.4%). These results could have important implications with respect to transport modeling. If the multiple-mobility fractions observed here are also present in the field, transport predictions based on classical modeling approaches that incorporate mobilities from batch sorption experiments are likely to be in error.

*E-mail: fjeld@clemson.edu
†Current address: Radian Corporation, 1093 Commerce Park Drive, Suite 100, Oak Ridge, Tennessee 37830.
‡Current address: Nuclear Regulatory Commission, Mail Stop TWFN 8-A-33, Washington, D.C. 20555.
§Current address: 500 Stanyon Street, San Francisco, California 94117-1869.
||Current address: Department of Chemistry, Hartwick College, Miller Hall, Oneonta, New York 13820.

I. INTRODUCTION

The Subsurface Disposal Area (SDA) within the Radioactive Waste Management Complex (RWMC) at the Idaho National Engineering and Environmental Laboratory (INEEL) contains shallow pits, soil vaults, and trenches where a variety of low-level, mixed, and transuranic wastes are buried. Among the radiological contaminants in the wastes[1,2] (Table I) are particularly large amounts of plutonium, americium, and uranium. The Snake River Plain aquifer is located ~180 m below the RWMC, and reliable models of radionuclide transport in the subsurface are needed for evaluating human health risk through the groundwater pathway. The vadose zone between the waste site and the aquifer consists of a layered sequence of fractured volcanic rocks (primarily basalts) and sedimentary interbeds. Modeling contaminant transport from the SDA to the aquifer is difficult because the system is highly heterogeneous, and there is significant uncertainty in both the hydrological conditions and the geochemical interactions that affect contaminant transport. To reduce uncertainties in predictions of subsurface transport, a major program known as the Integrated Large-Scale Aquifer Pumping and Infiltration Tests was undertaken.[3] However, the suite of tracers (^{75}Se, ^{85}Sr, ^{160}Tb, and bromide) was limited because of regulatory and cost constraints and included only one of the contaminants of concern (strontium). Consequently, laboratory data were needed to characterize the geochemical behavior of selected actinides and fission/activation products. The existing base of data for INEEL was limited to ^{90}Sr and ^{137}Cs (Refs. 4, 5, and 6), and laboratory column tests and batch tests were conducted with ^{60}Co, ^{90}Sr, ^{137}Cs, ^{233}U, ^{239}Pu, and ^{241}Am. Presented here are the results of laboratory column tests to characterize the mobilities of these radionuclides in basalt and sedimentary interbed from the site.

TABLE I

Estimated Inventory of the Principal Radiological Contaminants Buried at the RWMC*

Radionuclide	Activity (Ci)	Mass (kg)
^{3}H	1 400 000	0.15
^{14}C	12 000	2.8
^{59}Ni	6 200	82
^{63}Ni	1 100 000	19
^{60}Co	4 000 000	3.5
^{90}Sr	450 000	3.4
^{99}Tc	180	10
^{137}Cs	600 000	7.1
^{234}U	65	10
^{235}U	5	2 400
^{238}U	110	330 000
^{238}Pu	2 400	0.14
^{239}Pu	64 000	1 000
^{240}Pu	15 000	64
^{241}Pu	390 000	3.8
^{241}Am	150 000	43

*Reference 2. Measurements are not corrected for decay.

II. EXPERIMENTAL METHODS

II.A. Materials

Experiments were performed with basalt and interbed material from the INEEL site. The basalt was from a boulder removed from one of the burial pits at the RWMC. The sample was crushed and sieved, and the fraction >250 μm was used in the experiments. Sedimentary interbed was obtained from an uncontaminated region adjacent to the RWMC. This unconsolidated material was composited from core samples collected at five different depths ranging from 50 to 120 m and was sieved to the size fraction <250 μm. The physical and chemical characteristics of the two subsurface materials are given in Table II. The primary minerals in the sand fraction (>50 μm) of both materials were pyroxene (30 to 50%) and plagioclase (30 to 50%), with lesser amounts of quartz (in the interbed only), olivine, and magnetite. The primary minerals in the clay fraction (<0.002 μm) of interbeds from this area are vermiculite, mica, and montmorillonite. The interbed material had a higher cation exchange capacity (17 meq/100 g) than the basalt (6 meq/100g).

A synthetic groundwater (SGW) was formulated that approximated the actual major ion concentrations as determined from analysis of field samples.[7] The composition of the SGW is given in Table III. Spiked SGW was produced by adding acidic solutions of the radionuclides to the SGW and adjusting the pH to 8.00 $\pm$ 0.05 with 0.1 *N* NaOH. The chemical form of these solutions is given in Table IV. The radionuclide concentration ranged from 10 to 100 Bq/ml in the spiked SGW for each radionuclide. The final ionic strength of the spiked SGW was typically 0.004 *M*. Each spike contained a beta-emitting activation or fission product and an alpha-emitting actinide. Hydrogen-3 was used as a nonreactive tracer in each column to monitor for channeling.

II.B. Column Transport Studies

The column apparatus (Fig. 1) consisted of reservoirs for SGW and spiked SGW, a peristaltic pump,[a] the column packed with either basalt or interbed, and a

[a]The pump was a Masterflex Model 7550-90.

TABLE II

Physical and Chemical Characteristics of the Basalt and Sedimentary Interbed Samples as Measured by the Clemson University Agronomy and Soils Department

Characteristic	Basalt	Composite Sedimentary Interbed
Dithionite-citrate buffer extractable iron oxide (%Fe_2O_3)	---	1.77
NH_4OAc extractable Mn (ppm)	1.0	1.9
Total cation exchange capacity (meq/100 g)	6.05	17.4
Particle size distribution (μm)		
>250	84%	40%
100 to 250	4%	21%
50 to 100	1%	13%
2 to 50	8%	22%
<2	3%	4%
Bulk density ($g \cdot cm^{-3}$)	1.50 to 1.73	1.65 to 1.78
Porosity (n)	0.44 to 0.52	0.39 to 0.45
Major minerals	Pyroxene	Montmorillonite
	Plagioclase	Mica
	Olivine	Vermiculite

TABLE III

Chemical Composition of the SGW

Constituent	Concentration (mg/ℓ)
Ca^{2+}	28.5
K^+	9.8
Mg^{2+}	8.3
Na^+	17.0
Cl^-	41.3
SO_4^{2-}	23.4
HCO_3^-	89.3
F^-	0.5
H_2SiO_2	22.0
pH	8.0
Ionic strength (mol/ℓ)	0.004

TABLE IV

Chemical Makeup of the Radionuclide Sources Used to Prepare the Spiked SGW

Radionuclide	Chemical Form	Solution
^3H	HTO	H_2O
^{60}Co	$CoCl_2$	0.5 *M* HCl
^{90}Sr	$SrCl_2$	0.5 *M* HCl
^{137}Cs	CsCl	0.1 *M* HCl
^{233}U	$UO_2(NO_3)_2$	0.1 *M* HCl
^{239}Pu	$Pu(NO_3)_4$	4.0 *M* HNO_3
^{241}Am	$AmCl_3$	0.1 *M* HCl

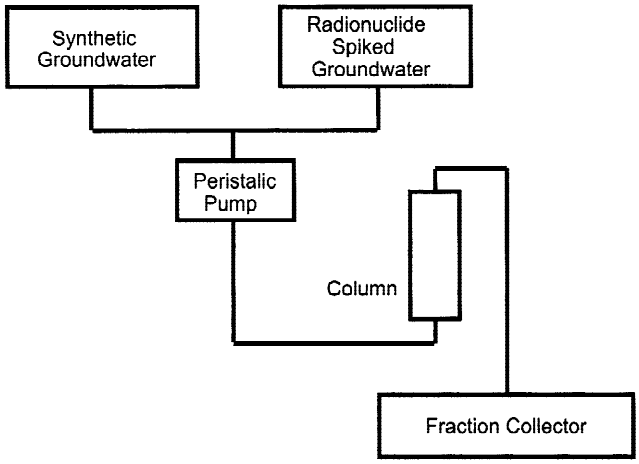

Fig. 1. Experimental apparatus.

fraction collector.[b] The column design was based on Relyea[8] to ensure that dispersion would not significantly affect contaminant travel time. The columns were constructed of polyvinylchloride cylinders with a 2.6-cm inner diameter and 15.2-cm length with bolted flanges at each end. Basalt columns were wet packed by adding crushed basalt in ~5-g increments and tamping lightly with a rod. Interbed columns were dry packed 1 cm at a time and compacted by lightly tapping the column on the bench top. The bulk densities of the packed columns ranged from 1.50 to 1.73 g/cm^3 for basalt and 1.65 to 1.78 g/cm^3 for sedimentary interbed. The porosity of

[b] An Eldex Universal Fraction Collector.

the packed columns ranged from 0.43 to 0.52 for basalt and 0.39 to 0.45 for sedimentary interbed. The pore volume was ~30 to 40 cm^3.

The spiked and unspiked SGW was introduced at the bottom of the vertically oriented columns, and effluent fractions were collected at the top. Analyses of the effluent fractions were performed with an alpha/beta-discriminating liquid scintillation counter.[c] This made it possible, in a single test, to simultaneously measure ^3H betas, higher-energy betas from an activation or fission product, and alphas from an actinide. The alpha/beta-emitting pairs were $^{233}U/^{60}Co$, $^{239}Pu/^{90}Sr$, and $^{241}Am/^{137}Cs$. In the $^{239}Pu/^{90}Sr$ experiments, ^3H was introduced as a separate spike that was followed by the $^{239}Pu/^{90}Sr$ spike because of ^{241}Pu contamination in the ^{239}Pu solution. Plutonium-241 has a beta particle with an endpoint energy (21.6 keV) that is indistinguishable from the ^3H beta particle, which has an endpoint energy of 18.6 keV.

The column tests were performed at least in duplicate for each set of alpha/beta emitters and each type of matrix. Results from a total of 15 column experiments are presented here. The test procedure was as follows. First, the unspiked SGW was pumped through the column for a 24-h equilibration period. Then, the spiked SGW containing the alpha/beta pair and ^3H (except as noted earlier) was introduced into the column as a finite step of ~1 pore volume in width. Following the spike, the column was washed with ~200 pore volumes of unspiked SGW. With one exception (basalt column 2), the volumetric flow rate was 1 ml/min, and the corresponding mean linear velocities ranged from 0.0065 to 0.0082 cm/s. The column effluent was collected in 3- to 20-ml fractions from which 1-ml aliquots were analyzed with the liquid scintillation counter for a 10-min count time. Elution profiles, i.e., normalized effluent concentration versus time [as displaced pore volume (DPV), which is the integrated volumetric flow divided by the pore volume], were plotted for each radionuclide.

II.C. Data Analysis

Attempts were made to fit three conventional one-dimensional (1-D) advection/dispersion/sorption transport models (equilibrium, one-site kinetic, and two-site equilibrium) to the data using the CXTFIT software package.[9] Originally, the objective of the fitting effort was to determine transport parameters such as dispersion coefficients, retardation factors, sorption rate constants, etc. The fits of the equilibrium model to ^3H data were good, and the CXTFIT code was used to obtain dispersion coefficients. This was accomplished by specifying the width of the contaminant step and the mean linear velocity (both of which are experimental control variables) and allowing the program to converge to the best estimate of dispersion coefficient. However, the fits for the other radionuclides were poor and thus did not provide a reliable means for providing a quantitative characterization of their mobilities. Consequently, the decision was made to characterize mobilities using the moments method.[10] In this approach, mean travel times are calculated by the following (see Nomenclature on p. 106):

$$\bar{t} = \frac{\int tC(t)\,dt}{\int C(t)\,dt} - \frac{T}{2} \quad , \tag{1}$$

where $C(t)$ is aqueous phase concentration in the effluent and T is the width of the finite step spike. The retardation factor R was calculated as the ratio of the mean travel time of the radionuclide of interest, $\bar{t}_x$, to the mean travel time of ^3H, $\bar{t}_H$,

$$R_x = \bar{t}_x / \bar{t}_H \quad . \tag{2}$$

Aqueous recovery f_R was calculated from

$$f_R = \frac{\int C(t)\,dt}{C_0 \cdot T} \quad , \tag{3}$$

where C_0 is the radionuclide concentration in the spike. Aqueous recovery is typically expressed as a percentage.

Some of the columns with aqueous recoveries <100% underwent further testing. Some were scanned with a NaI(Tl) detector to determine the location of gamma-ray emitters at the end of the elution period. The detector was placed behind a 5-cm-thick lead shield that had a 1- × 10-cm slit. The column was positioned so as to be scanned in contiguous 1-cm segments. Also, the basalt and interbed in selected columns were acid washed. Approximately 3 pore volumes (90 ml) of 2.0 *M* HNO_3 was pumped through the column, and the effluent was collected. A 1-ml aliquot of this effluent was analyzed.

III. RESULTS AND DISCUSSION

III.A. Basalt

Elution profiles for basalt are presented in Figs. 2a through 2f. Each graph contains profiles for ^3H and one of the radionuclides of interest. Transport parameters calculated from the elution profiles are presented in Table V for ^3H and in Table VI for the radionuclides of interest.

All of the ^3H elution profiles were similar in that they were approximately symmetric and showed no evidence of channeling. Aqueous recoveries ranged from 91 to 112%, and retardation factors ranged from 0.94 to 1.09. The dispersion coefficients ranged from 0.0006 to 0.0021 cm^2/s.

The elution profiles for uranium, cesium, and strontium (Figs. 2a, 2b, and 2c, respectively) were similar in

[c]Model 1415 manufactured by Perkin Elmer Wallac.

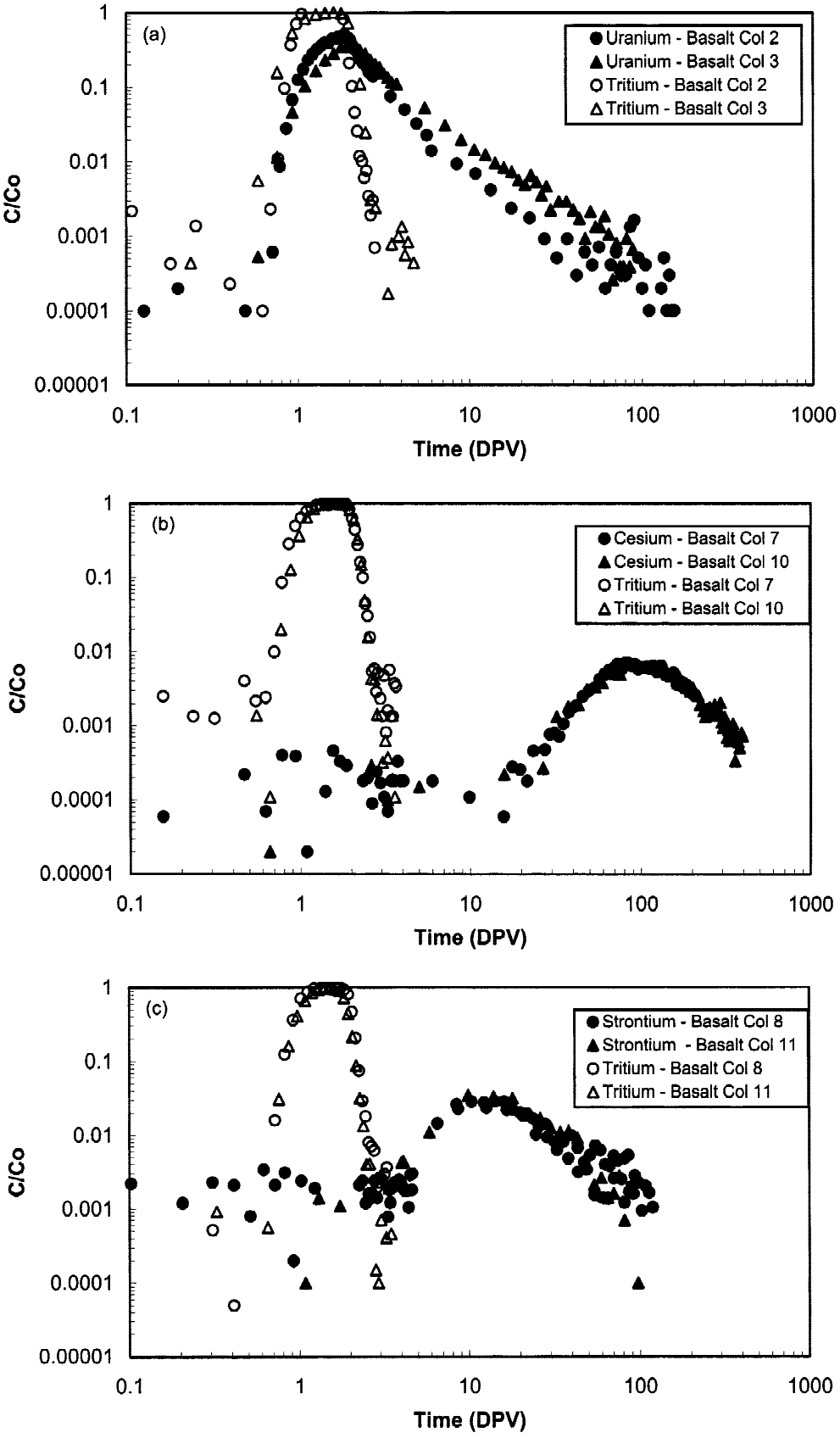

Fig. 2. Elution profiles for basalt columns. (Figure continues on facing page.)

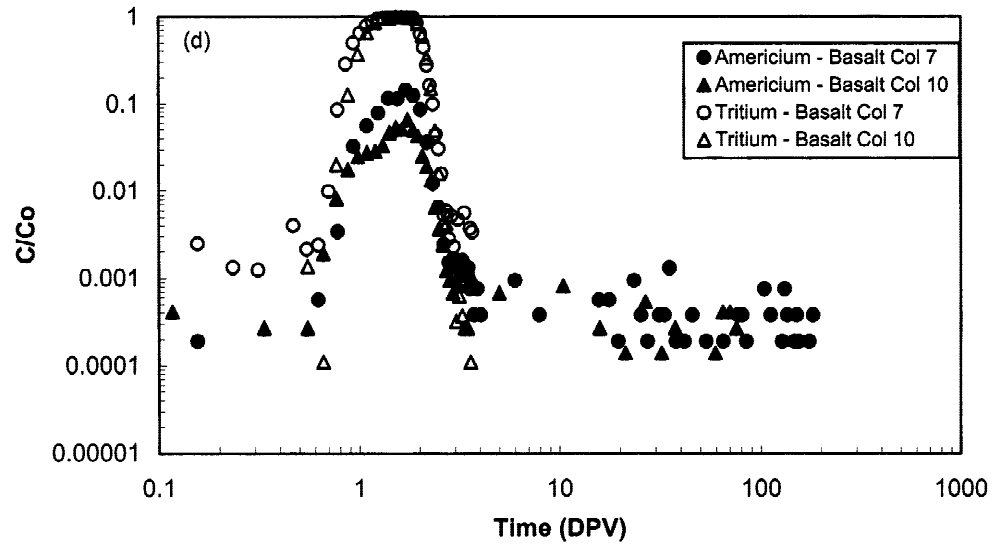

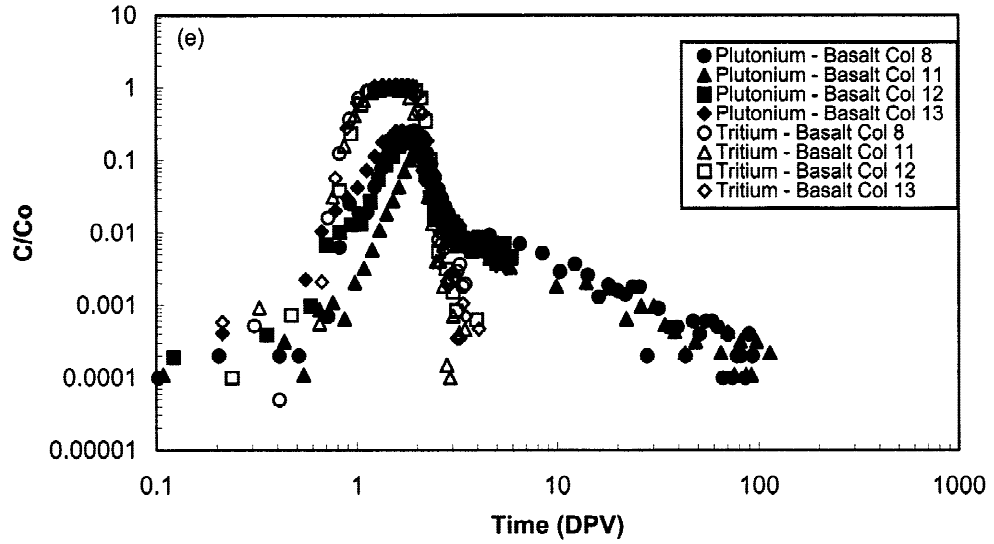

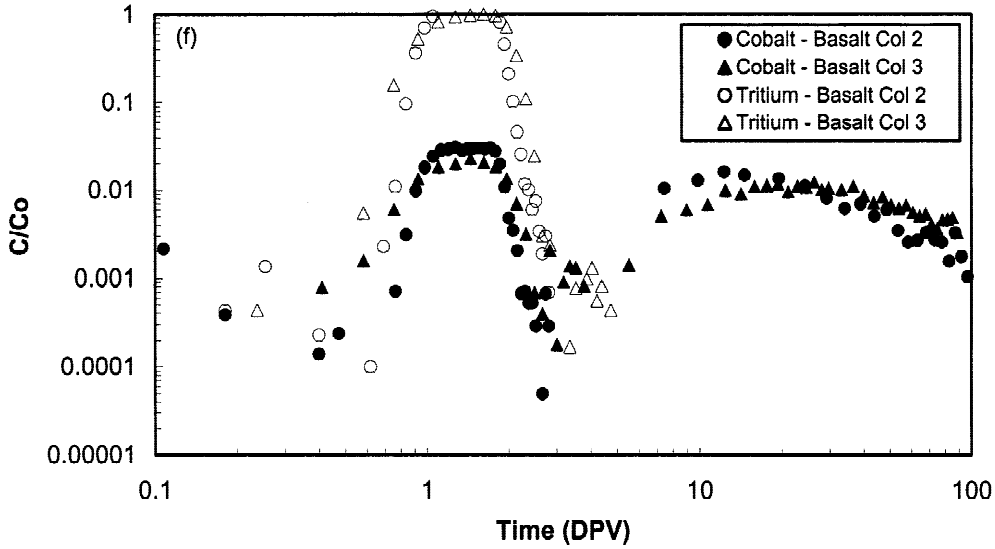

Fig. 2. Continued.

TABLE V

Physical Characteristics of the Basalt Columns and Parameters Obtained by Fitting the 1-D Advection/Dispersion Equation to the ^{3}H Data

Basalt Column Number	pH	n	ρ (g/cm^3)	ν (cm/s)	T (DPV)	Aqueous Recovery f_R (%)	$\bar{t}$ (DPV)	Fitted Parameters for ^{3}H (Equilibrium Model)		
								D (cm^2/s)	R	Correlation Coefficient
2	8.02	0.52	1.50	0.0123	0.97	91	0.95	0.0006	0.95	0.98
3	8.09	0.44	1.73	0.0073	1.15	101	1.03	0.0021	0.94	1.00
8	8.04	0.49	1.62	0.0065	1.12	97	1.02	0.0009	0.95	1.00
11	8.05	0.47	1.65	0.0069	0.95	102	1.13	0.0014	1.01	1.00
12	8.13	0.43	1.69	0.0074	1.02	110	1.10	0.0010	1.09	0.98
13	8.09	0.44	1.64	0.0072	0.99	112	1.06	0.0009	1.06	0.95
7	8.12	0.49	1.60	0.0066	1.14	100	1.04	0.0014	0.96	1.00
10	8.12	0.46	1.62	0.0069	1.09	98	1.8	0.0012	1.04	1.00

TABLE VI

Aqueous Recoveries and Corresponding Retardation Factors for the Basalt Columns

Basalt Column Number	Radionuclide	Aqueous Recovery f_R (%)	R	Radionuclide	Aqueous Recovery f_R (%)	R
2	^{60}Co	3.0	1[a]	^{233}U	99	5.1
	^{60}Co	59	34[b]	−−−	−−−	−−−
3	^{60}Co	2.3	0.9[a]	^{233}U	106	6.1
	^{60}Co	74	34[b]	−−−	−−−	−−−
8	^{90}Sr	93	33	^{239}Pu	29	4.3
11	^{90}Sr	118	25	^{239}Pu	17	5
12	−−−	−−−	−−−	^{239}Pu	17	1.3
13	−−−	−−−	−−−	^{239}Pu	24	1.2
7	^{137}Cs	67	70	^{241}Am	12	2.6
10	^{137}Cs	90	88	^{241}Am	7.0	5.8

[a]First peak in elution profile.
[b]Second peak in elution profile.

that each was characterized by a single peak containing essentially all of the activity that was in the spike within the limits of experimental uncertainty (estimated to be ±15% from the ^{3}H data). The uranium mobility was very high ($\bar{R}$ = 5.6), and the average aqueous recovery was 103%. Cesium mobility was much lower ($\bar{R}$ = 79). Aqueous recovery for one of the cesium columns was only 67%; however, the test was terminated before all of the peak appeared. In the replicate, the duration of the test was increased, and the aqueous recovery was 90%. The strontium mobility ($\bar{R}$ = 29) was between that of uranium and cesium, and the average aqueous recovery was 105%. These results suggest that uranium, cesium, and strontium are present as single species. For uranium, the likely species are hydroxides and/or carbonate complexes of the UO_2^{2+} cation.[11–13] Such complexes are either neutral or anionic and have a low affinity for the solid phase. This is consistent with the high mobility observed in the columns. For cesium and strontium, retardation is likely due to interaction of the Cs^+ and Sr^{2+} cations with clay minerals in the basalt sample. The greater retardation of cesium compared to strontium is consistent with results from batch partitioning experiments.[14,15] This is commonly attributed to irreversible retention of cesium between structural layers of clay minerals such as mica and vermiculite.[16] The moderate degree of retardation of both is consistent with the relatively low cation-exchange capacity of the basalt and the relatively small

surface area associated with the basalt size fraction used in the columns.

The elution profiles for americium, plutonium, and cobalt (Figs. 2d, 2e, and 2f, respectively) were substantially different from those for uranium, cesium, and strontium in that they suggest multiple forms having distinctly different mobilities. For americium and plutonium, a small fraction of the activity in the spike had a high mobility, but the majority of the activity did not appear within 200 DPV. The average retardation factors and recoveries were $\bar{R} = 4.2$ and $f_R = 9.5\%$ for americium and $\bar{R} = 3.0$ and $f_R = 22\%$ for plutonium. Cobalt was particularly intriguing because it had a small ($f_R = 2.6\%$), high-mobility ($\bar{R} = 1$) fraction; a large ($f_R = 67\%$), moderate-mobility ($\bar{R} = 34$) fraction; and the remainder ($f_R \approx 30\%$) retained in the column. It is interesting to compare the elution profiles of the high-mobility fractions of cobalt, americium, and plutonium to those for ^{3}H. The cobalt profile appears to have an identical shape to that for ^{3}H while those for americium and plutonium differ. The leading edges of the americium and plutonium profiles are somewhat irregular and slightly retarded compared to ^{3}H, especially for plutonium. For cobalt, this suggests a soluble species or a small particulate form. For americium and plutonium, the implication is not known. However, since americium and plutonium(IV) generally have very low solubilities at high pH, it is possible that particulate forms may have played a role in their behavior. For plutonium, the interpretation is clouded by the likely presence of a mix of plutonium (IV) and plutonium (V) in the spike.

The gamma-ray scans showed the ^{60}Co, ^{137}Cs, and ^{241}Am remaining in the column to be approximately uniformly distributed throughout its length. Acid leaching of the basalt yielded total recoveries of 98% for ^{137}Cs (basalt column 10), 89% for ^{239}Pu (basalt column 11), and 82% for ^{241}Am (basalt column 10).

Fried et al.[17] and Thompson[18] have also observed low- and high-mobility forms of plutonium and americium under geochemical conditions similar to those studied here. Fried et al. performed two types of experiments with volcanic tuff from Los Alamos National Laboratory (LANL). In the first, plutonium and americium were deposited in a depression on the top of a block of tuff. After several "rain-drought" cycles in which the block was showered with water and allowed to dry, cores were extracted from the block. Each core showed two zones of activity as a function of depth. There was a low-mobility zone close to the site of deposition that contained the majority of the plutonium and a high-mobility zone some distance away that contained <1% of the original activity. Small, high mobility fractions were also observed in column tests with crushed (and washed) tuff. From these experiments, it was estimated that 1% of the plutonium had a mobility that was 25 000 times higher than the bulk of the plutonium. Thompson peformed column tests with crushed tuff and groundwater ("J-13") from the Nevada Test Site, which is similar to the SGW used in our experiments. He observed fractions of plutonium, americium, and neptunium to travel through the columns at approximately the same speed as tritium. For plutonium, the high-mobility fraction depended on the oxidation state. It was as high as 70% for Pu(V) and/or Pu(VI), but it was generally <10% for Pu(IV). The behavior of americium was similar to that of Pu(IV), and the behavior of neptunium was similar to that of Pu(V)/Pu(VI). High mobility forms of plutonium have also been observed in field studies. Penrose et al.[19] found elevated plutonium and americium concentrations in a small aquifer at LANL. All of the plutonium and part of the americium was associated with particulate material in the 0.025- to 0.45-μm size range. Although Penrose et al. attributed the presence of the radionuclides to particulate transport through the aquifer, Marty et al.[20] subsequently made a case for infiltration of surface water. Buddemeier and Hunt[21] and Kersting et al.[22] observed high-mobility transport of radionuclides at the Nevada Test Site. In the most recent study by Kersting et al., the high-mobility forms of cobalt, cesium, europium, and plutonium were almost all a particulate form. McCarthy et al.[23] concluded that high-mobility forms of americium at the Oak Ridge National Laboratory were due to natural organic matter.

There are at least three possible explanations for the observed high mobility of ^{60}Co, ^{239}Pu, and ^{241}Am. These are (a) association with a mobile particulate phase, (b) formation of a mobile complex, or (c) kinetically limited sorption. Experiments were performed to test for each of these three mechanisms. First, to investigate the possibility of particulate transport, the spiked groundwater influent solution was double filtered through 0.1-μm SUPOR 100 polysulfone filters, and ^{239}Pu concentrations were measured before the filtrations and after each of the two filtrations. There was no loss of activity in the second filter, which indicates that plutonium was not sorbed by the filter material. Approximately 25% of the ^{239}Pu in the spike solution was removed by the first filter. This fraction remained constant over a 20-h period following preparation of a pH-adjusted spike. Effluents from plutonium and americium columns were similarly filtered. The first filter removed 5 to 22% of the ^{239}Pu and 28% of the ^{241}Am. Although not conclusive evidence of particulate transport, these results indicate the presence of suspended particles in both the influent and the effluent, they are supportive of a particulate transport hypothesis for ^{239}Pu and ^{241}Am, and they are consistent with the findings of Thompson.[18] Similar filtrations were not performed for ^{60}Co; however, it is also known to form and strongly sorb to suspended particles.[24–27] Thus, particulate transport is a possible explanation for the cobalt high-mobility fraction as well.

Plutonium-239 and ^{241}Am are known to form neutral or negatively charged complexes with carbonate.[11,28,29] To examine the possibility of enhanced transport of plutonium due to the formation of negatively charged

TABLE VII

Effect of Bicarbonate on Plutonium Recovery

Eluent	HCO_3^- Concentration (mg/ℓ)	f_R (0 to 4DPV) (%)	f_R (0 to 60 DPV) (%)
SGW without added carbonate or bicarbonate salts	Low[a]	12	59
SGW	90	30	52
SGW with high bicarbonate	1800	58	78

[a]Due to CO_3^{2-} from the atmosphere and possibly carbonate/bicarbonate salts leached from the basalt.

carbonate complexes, a set of experiments was conducted in which the bicarbonate concentration was varied. The eluent solutions for these experiments were as follows: (a) SGW without added carbonate or bicarbonate salts, (b) SGW, and (c) SGW with 20 times the base bicarbonate concentration. The spikes were allowed to equilibrate for 24 h before the test was begun. The results are summarized in Table VII, where the fractional recoveries are given for the 0- to 4-DPV time period and for the entire elution period of ~60 DPV. The recovery for the 0- to 4-DPV time period increased dramatically with increasing bicarbonate concentration. Though not conclusive, this is consistent with the carbonate complexation hypothesis regarding enhanced transport of plutonium. The recoveries for each of these experiments exceeded 50%. For the SGW, this is a factor of 2 higher than in the previous experiments (basalt columns 8 and 11 through 13) and is possibly due to differences in the preparation and/or aging of the spike solution.

Finally, the effect of flow rate on ^{241}Am mobility was examined. The results are given in Fig. 3. As the flow rate was increased from 0.1 to 10 ml/min, the high-mobility fraction increased from 1 to 43%. This could be due either to an increase in the release of particles with increased water velocity (because of increased shear forces) or to a decrease in the sorbed fraction (if sorption is kinetically limited).

III.B. Sedimentary Interbed

Elution profiles for sedimentary interbed are presented in Figs. 4a through 4f. As for basalt, the interbed graphs contain profiles for ^3H and one of the radionuclides of interest. Transport parameters calculated from the elution profiles are presented in Table VIII for ^3H and in Table IX for the radionuclides of interest. As for basalt, the ^3H elution profiles for interbed were all approximately symmetric and showed no evidence of

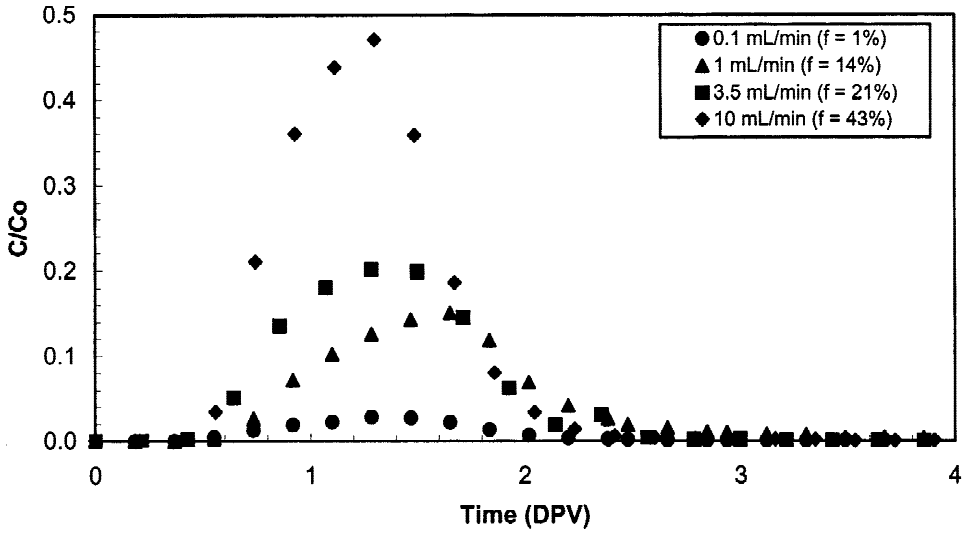

Fig. 3. Elution profiles for ^{241}Am for volumetric flow rates from 0.1 to 10 ml/min. The legend value in parentheses is the aqueous recovery.

TABLE VIII

Physical Characteristics of the Interbed Columns and Parameters Obtained by Fitting the 1-D Advection/Dispersion Equation to the ^{3}H Data

Interbed Column Number	pH	n	ρ (g/cm^3)	ν (cm/s)	T (DPV)	Aqueous Recovery f_R (%)	$\bar{t}$	Equilibrium Model		
								D (cm^2/s)	R	Correlation Coefficient
1	8.48	0.45	1.65	0.0072	1.13	110	1.13	0.0008	1.05	0.98
2	8.46	0.43	1.69	0.0075	1.18	106	1.13	0.0006	1.03	0.99
6	8.36	0.40	1.78	0.0080	1.42	99	1.25	0.0009	1.04	1.00
7	8.57	0.41	1.74	0.0079	1.09	101	1.13	0.0008	1.07	1.00
9	8.51	0.39	1.78	0.0082	1.13	96	1.11	0.0013	1.04	1.00
5	8.62	0.41	1.69	0.0072	1.37	93	1.20	0.0022	1.01	0.98
8	8.72	0.41	1.72	0.0077	1.22	99	1.16	0.0005	1.05	1.00

TABLE IX

Aqueous Recoveries and Corresponding Retardation Factors for the Interbed Columns

Interbed Column Number	Radionuclides	Aqueous Recovery, f_R (%)	R	Radionuclides	Aqueous Recovery, f_R (%)	R
1	^{60}Co	1.1	>800[a]	^{233}U	96	31
2	^{60}Co	3.9	~1	^{233}U	101	30
6	^{90}Sr	---	>200[b]	^{239}Pu	1.1	~3
7	^{90}Sr	---	>200[b]	^{239}Pu	2.4	~3
9	^{90}Sr	---	>200[b]	^{239}Pu	1.4	~3
5	^{137}Cs	---	>800[a]	^{241}Am	---	~800[a]
8	^{137}Cs	---	>200[b]	^{241}Am	---	>200[b]

[a]As determined from the contaminant remaining on the column by gamma-ray scans.
[b]As determined from the contaminant not appearing in the aqueous effluent.

channeling. Aqueous recoveries for ^{3}H ranged from 93 to 110%, retardation factors ranged from 1.01 to 1.07, and dispersion coefficients ranged from 0.0005 to 0.0022 cm^2/s.

Uranium (Fig. 4a) was the only radionuclide, other than ^{3}H, with essentially 100% recovery within the 200-DPV sampling period. Its mobility in interbed ($\bar{R} = 30$) was lower than in basalt. This is consistent with interbed's larger cation exchange capacity and larger surface area compared to basalt. To assist in distinguishing between very low breakthrough and no breakthrough, the elution profiles for cesium, strontium, americium, plutonium, and cobalt are also plotted on an expanded linear scale in Figs. 5a through 5e, respectively. For cesium (Figs. 4b and 5a) and strontium (Figs. 4c and 5b), there was no breakthrough within the first 200 DPV. However, for plutonium (Figs. 4e and 5d) and cobalt (Figs. 4f and 5e), there was evidence of small, high-mobility fractions of each. The average recoveries were 1.6% for three plutonium columns and 2.5% for two cobalt columns. Although close examination of the americium data (Figs. 4d and 5c) suggests the possibility of a high-mobility fraction, the signal was not sufficiently above background for confirmation. The gamma-ray scans of the columns showed ^{60}Co, ^{137}Cs, and ^{241}Am to be located within 3 to 4 cm of the inlet (Fig. 6), suggesting high retardation factors. A travel distance of <4 cm during the ~100 h of the column experiments implies a retardation factor in excess of 600. This, in turn, implies a distribution coefficient in excess of 3200, which is consistent with the results of other studies.[16,30] Acid leaching of the interbed yielded total recoveries of 112% for ^{90}Sr (interbed

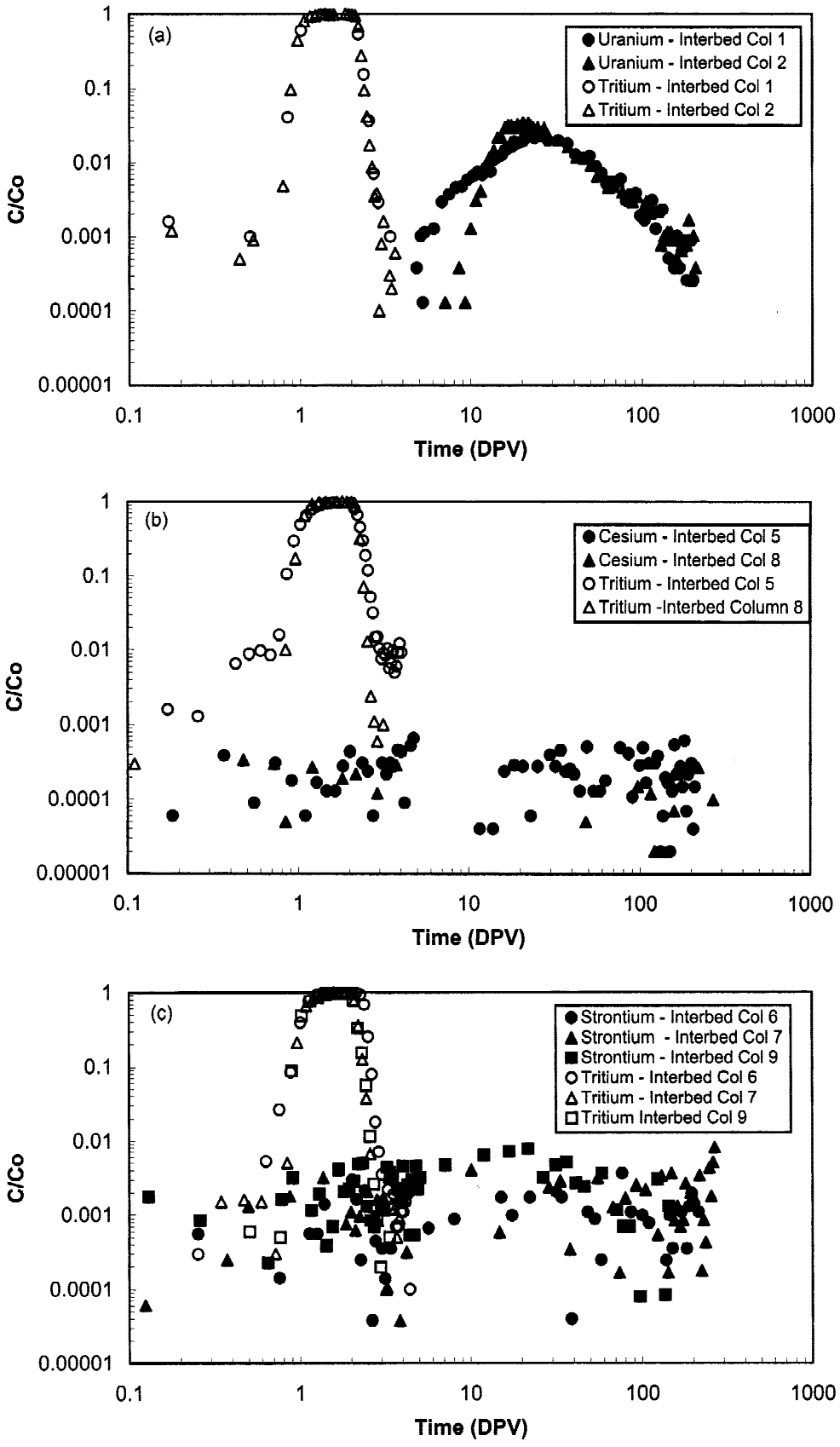

Fig. 4. Elution profiles sedimentary interbed columns. (Figure continues on facing page.)

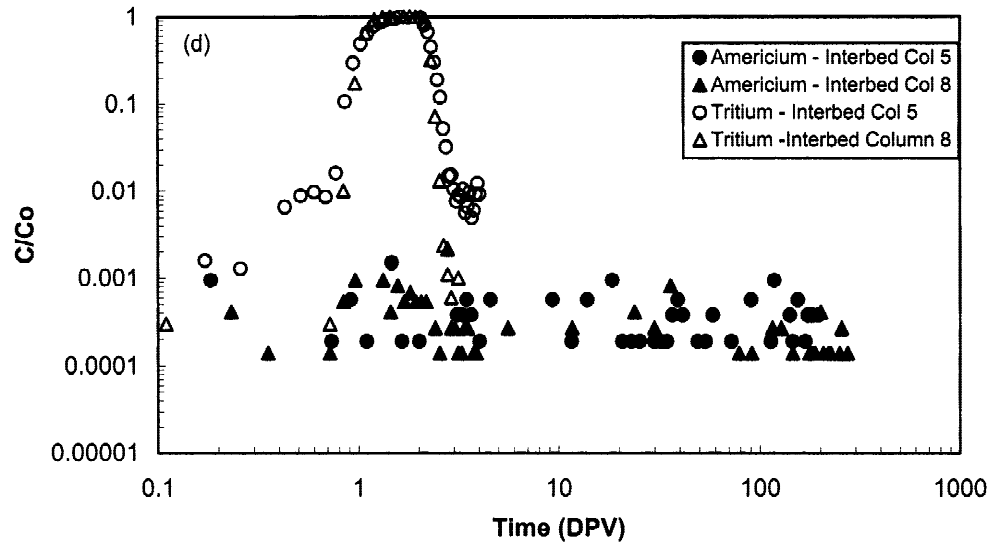

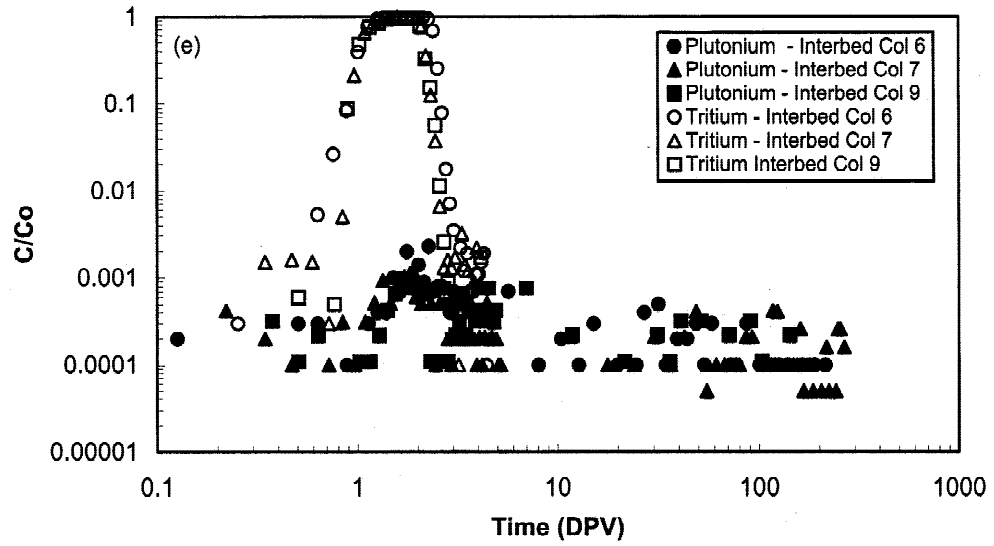

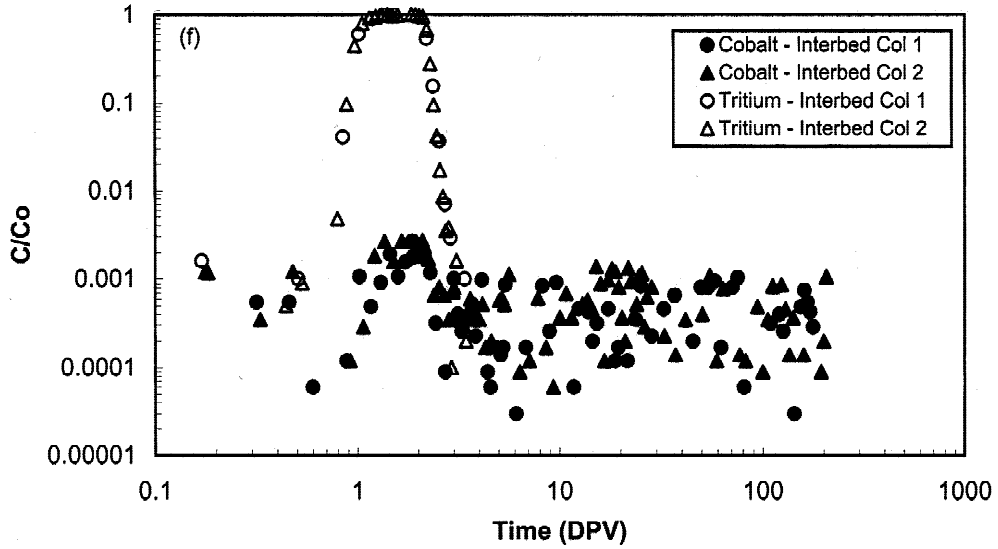

Fig. 4. Continued.

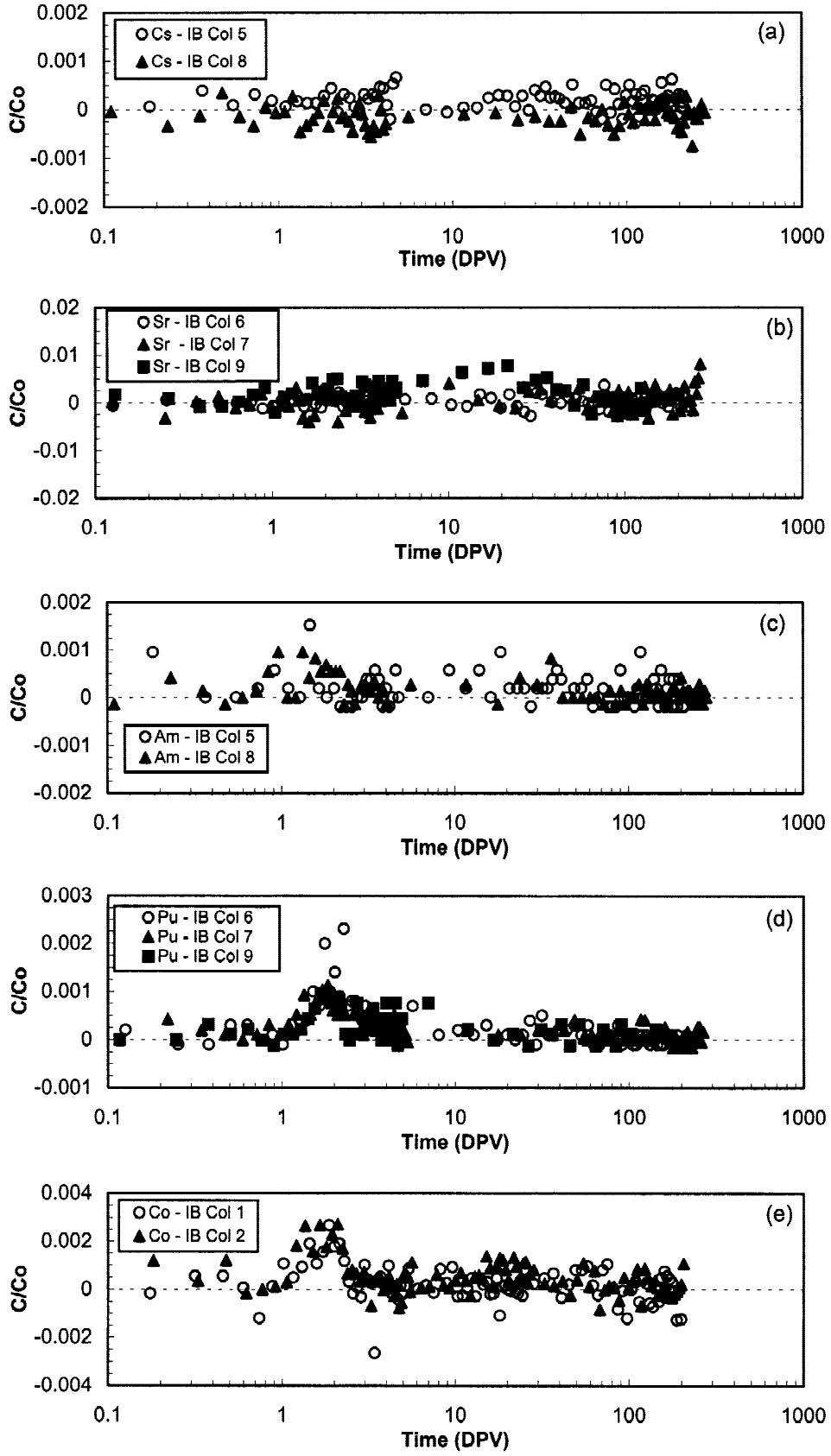

Fig. 5. Elution profiles for sedimentary interbed with an expanded scale on the ordinate.

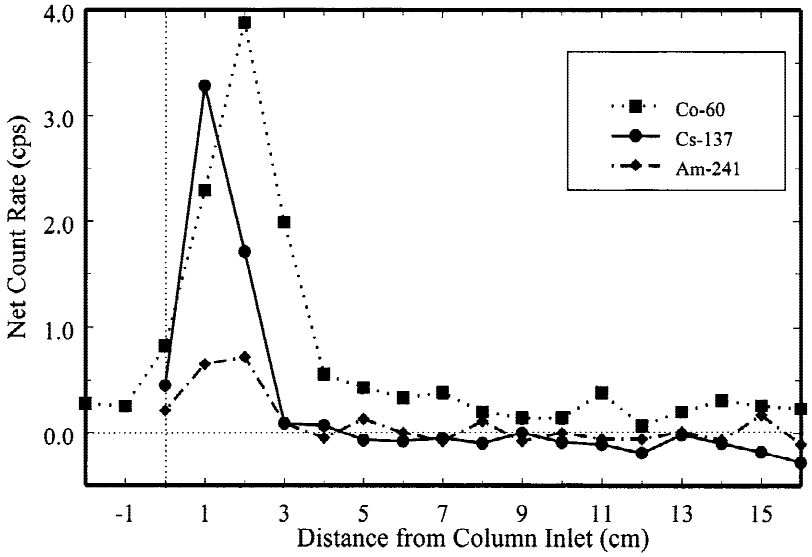

Fig. 6. Spatial distribution of ^{60}Co(interbed column 2), ^{137}Cs (interbed column 5), and ^{241}Am (interbed column 5) in interbed columns as determined from a gamma-ray scan with 1-cm resolution. The values are connected point to point to assist in distinguishing among the sets of data.

column 9), 49% for ^{137}Cs (interbed column 8), 63% for ^{239}Pu (interbed column 9), and 83% for ^{241}Am (interbed column 8).

III.C. Transport Modeling Implications

Most models for predicting the subsurface transport of contaminants consist of a hydrological component to determine the direction and speed of water flow and a geochemical component to determine the extent to which the subsurface material retards contaminant movement with respect to the water. The effect of geochemical interactions is usually inferred from batch experiments and incorporated into the model as a single retardation factor. Whereas batch tests can provide useful data for modeling the transport of a contaminant that is present in a single physical/chemical form, they are not useful for a contaminant that is present in two or more forms having different mobilities. This is because multiple forms are masked in batch sorption experiments. In this study, tritium, uranium, strontium, and cesium were present in a single form; but plutonium, americium, and cobalt were observed to have multiple forms.

However, it is necessary to exercise caution in attempting to extrapolate observations from our laboratory columns to draw conclusions about transport under the complex conditions encountered in the field. There are a number of reasons for this. One is that the mean linear velocity in the laboratory columns was between two and three orders of magnitude greater than that typical of the subsurface. Evidence of a velocity dependence can be seen in Fig. 3, where the high-mobility fraction of ^{241}Am increased with increasing mean linear velocity. A second reason, which is specifically applicable to plutonium, is the effect of spike preparation on the plutonium oxidation state. It is well known that plutonium can be present as Pu(III), Pu(IV), Pu(V), and Pu(VI) simultaneously in natural waters. The plutonium oxidation state was neither controlled nor monitored in these experiments. Thus, it is likely that the oxidation state distribution varied somewhat from experiment to experiment. This variability may be the reason for the considerable difference in plutonium recoveries in basalt columns 8 and 11 through 13 and those in Table VII. A third reason is the possible difference between geochemical conditions in the field and those in the laboratory experiments. The laboratory columns are probably a reasonable approximation for the far field, where the geochemical conditions are not influenced by the waste. However, they are probably a poor approximation in the near field, where the constituents leaching from the waste are likely to affect both the aqueous chemistry and the reactive surfaces of the subsurface material.

IV. CONCLUSIONS

The principal objective of this study was to characterize the mobilities of ^{60}Co, ^{90}Sr, ^{137}Cs, ^{233}U, ^{239}Pu, and ^{241}Am in laboratory columns containing a sample of basalt and a composite of sedimentary interbeds from the Snake River Plain at INEEL. In basalt, the behavior of ^{90}Sr, ^{137}Cs, and ^{233}U was quite different from that of ^{60}Co, ^{239}Pu, and ^{241}Am. The column effluent curves for

the former were characterized by single peaks containing, within the limits of experimental uncertainty, all of the activity in the spike. The relative mobilities were ^{233}U ($\bar{R} = 5.6$) > ^{90}Sr ($\bar{R} = 29$) > ^{60}Co ($\bar{R} = 34$) > ^{137}Cs ($\bar{R} = 79$). The elution profiles for ^{60}Co, ^{239}Pu, and ^{241}Am suggest multiple physical/chemical forms with distinctly different mobilities. Although the majority of each radionuclide had intermediate or low mobility, they each had a high-mobility ($R < 3$) fraction ($f_R \approx 3\%$ for ^{60}Co, 25% for ^{239}Pu, and 10% for ^{241}Am). For ^{239}Pu and ^{241}Am, the remainder had low mobility ($R > 200$). For ^{60}Co, 67% appeared in a peak with $\bar{R} = 34$, and the remainder was retained in the column ($R > 200$). In interbed, mobilities were much lower than in basalt. Uranium-233 emerged from the column with $\bar{R} = 30$, while ^{90}Sr and ^{137}Cs did not appear within 200 DPV ($R > 200$). High-mobility fractions were observed for ^{60}Co ($f_R = 1$ to 4%) and ^{239}Pu ($f_R = 1.1$ to 2.4%). Based on gamma-ray scans, the majority of the ^{60}Co, ^{137}Cs, and ^{241}Am had retardation factors in excess of 600. Tests conducted to determine if the high-mobility fractions were due to particulate transport, formation of neutral or negative complexes, and kinetic limitations were inconclusive in that they were supportive of each of the hypothesized mechanisms.

These results could have important implications with respect to transport modeling. If the multiple-mobility fractions observed here are also present in the field, transport predictions based on classical modeling approaches that incorporate mobilities from batch sorption experiments are likely to be in error.

NOMENCLATURE

$C(0)$ = initial or influent aqueous-phase contaminant concentration (Bq/ℓ)

$C(t)$ = aqueous phase contaminant concentration (Bq/ℓ)

D = dispersion coefficient (cm^2/s)

f_R = aqueous recovery

n = porosity

R = retardation factor

$\bar{R}$ = mean retardation factor

T = width of finite step spike (s or DPV)

t = time (s or DPV)

$\bar{t}$ = mean travel time (s or DPV)

$\overline{t_H}$ = mean travel time for ^3H (s or DPV)

v = mean linear velocity (cm/s)

x = distance along the longitudinal column axis (m)

Greek

ρ = bulk soil density (kg/cm^3)

ACKNOWLEDGMENTS

This work was performed under contract C91-103410-KF-172-93 for EG&G Idaho, Inc. and LMITCo. The authors would like to thank the Clemson University Agronomy and Soils Department for conducting the basalt and interbed analyses.

REFERENCES

1. "A Comprehensive Inventory of Radiological and Nonradiological Contaminants in Waste Buried in the Subsurface Disposal Area of the INEL During the Years 1952–1983," INEL-95/031 (formerly EGG-WM-10903), Rev. 1, Idaho National Engineering Laboratory (1995).

2. B. H. BECKER, Idaho National Engineering and Environmental Laboratory, Personal Communication (1998).

3. M. E. NEWMAN and F. M. DUNNIVANT, "Results from the Large-Scale Aquifer Pumping and Infiltration Test: Transport of Tracers Through Fractured Media," INEL-95/146 and ER-WAG7-77, Idaho National Engineering Laboratory (1995).

4. J. A. DEL DEBBIO and T. R. THOMAS, "Transport Properties of Radionuclides and Hazardous Chemical Species in Soils at the Idaho Chemical Processing Plant," WINCO-1068 (1989).

5. D. B. HAWKINS and H. L. SHORT, "Equations for the Sorption of Cesium and Strontium on Soil and Clinoptilite," IDO-12046, Atomic Energy Commission, Idaho Operations Office (1965).

6. B. L. SCHMALZ, "Radionuclide Distribution in Soil Mantle of the Lithosphere as a Consequence of Waste Disposal at the National Reactor Testing Station," IDO-10049, Atomic Energy Commission, Idaho Operations Office (1972).

7. W. W. WOOD and W. H. LOW, "Aqueous Geochemistry and Diagenesis in the Eastern Snake River Plain Aquifer System, Idaho," *Geol. Soc. Am. Bull.*, **97**, 1456 (1986).

8. J. F. RELYEA, "Theoretical and Experimental Considerations for the Use of the Column Method for Determining Retardation Factors," *Radioac. Waste Manage. Nucl. Fuel Cycle*, **3**, 151 (1982).

9. J. C. PARKER and M. Th. VAN GENUCHTEN, "Determining Transport Parameters from Laboratory and Field Tracer Experiments," Virginia Agricultural Experiment Station, Bulletin 84-3, ISSN 0096-6088, Virginia Polytechnic Institute and State University (1984).

10. M. JIN, M. DELSHAD, V. DWARAKANATH, D. C. McKINNEY, G. A. POPE, K. SEPEHRNOORI, and C. E. TILBURG, "Partitioning Tracer Test for Detection, Estimation,

and Remediation Performance Assessment of Subsurface Nonaqueous Phase Liquids," *Water Resour. Res.*, **31**, *5*, 1201 (1995).

11. T. O. EARLY, G. K. JACOBS, and D. R. DREWES, "Geochemical Controls on Radionuclide Releases from a Nuclear Waste Repository in Basalt," in *Geochemical Behavior of Radioactive Waste*, American Chemical Society (1984).

12. B. S. JENSEN, "The Geochemistry of Radionuclides with Long Half-Lives: Their Expected Migration Behavior," Riso-R-430, Riso National Laboratory (1980).

13. L. L. AMES, J. E. McGARRAH, and B. A. WALKER, "Basalt Radionuclide Reactions: FY-1981 Annual Report," RHO-BW-CR-127-P, Pacific Northwest Laboratories (1981).

14. D. ISHERWOOD, "Geoscience Data Base Handbook for Modeling a Nuclear Waste Repository," NUREG/CR-0912, U.S. Nuclear Regulatory Commission (1981).

15. R. J. SERNE and J. F. RELYEA, "Waste Rock Interactions Technology Program: The Status of Radionuclide Sorption-Desorption Studies Performed by the WRIT Program," PNL-3997, Pacific Northwest Laboratory (1982).

16. M. G. M. BRUGGENWERT and A. KAMPHORST, "Survey of Experimental Information on Cation Exchange in Soil Systems," *Soil Chemistry: B. Physico-Chemical Models*, G. H. BOLT, Ed., Elsevier Scientific Publishing Company, New York (1979).

17. S. FRIED, A. M. FRIEDMAN, and R. WEEBER, "Studies of the Behavior of Plutonium and Americium in the Lithosphere," ANL-8096, p. 10, Argonne National Laboratory (1974).

18. J. L. THOMPSON, "Actinide Behavior on Crushed Rock Columns," *J. Radioanal. Nucl. Chem.*, **130**, *2*, 353 (1989).

19. W. R. PENROSE, W. L. POLZER, E. H. ESINGTON, D. M. NELSON, and K. A. ORLANDINI, "Mobility of ^{239}Pu and ^{241}Am Through a Shallow Aquifer in a Semiarid Region," *Environ. Sci. Technol.*, **24**, 228 (1990).

20. R. C. MARTY, D. BENNETT, and P. THULLEN, "Mechanism of Plutonium Transport in a Shallow Aquifer in Mortandad Canyon, Los Alamos National Laboratory, New Mexico," *Environ. Sci. Technol.*, **31**, 2020 (1997).

21. R. W. BUDDEMEIER and J. R. HUNT, "Transport of Colloidal Contaminants in Groundwater: Radionuclide Migration at the Nevada Test Site," *Appl. Geochem.*, **3**, 535 (1998).

22. A. B. KERSTING, D. W. EFURD, D. L. FINNEGAN, D. J. ROKOP, D. K. SMITH, and J. L. THOMPSON, "Migration of Plutonium in Ground Water at the Nevada Test Site," *Nature*, **397**, *7*, 56 (1999).

23. J. F. McCARTHY, W. E. SANFORD, and P. L. STAFFORD, "Lanthanide Field Tracers Demonstrate Enhanced Transport of Transuranic Radionuclides by Natural Organic Matter," *Environ. Sci. Technol.*, **32**, *24*, 3901 (1998).

24. A. SORATHESN, G. BRUSCIA, T. TAMURA, and E. G. STRUXNESS, "Mineral and Sediment Affinity for Radionuclides," CF-60-6-93, Oak Ridge National Laboratory (1960).

25. P. H. TEWARI, A. B. CAMPBELL, and W. LEE, "Adsorption of ^{60}Co(II) by Oxides from Aqueous Solution," *Can. J. Chem.*, **50**, 1642 (1972).

26. J. L. MEANS, D. A. CRERAR, M. P. BORCSIK, and J. O. DUGUID, "Adsorption of Co and Selected Actinides by Mn and Fe Oxides in Soils and Sediments," *Geochim. Cosmochim. Acta*, **42**, 1763 (1978).

27. V. MOULIN, N. LABONNE, and M. THEYSSIER, "Retention Properties of Silica Colloids Toward Actinides," *Proc. 3rd Int. Conf. Chemistry and Migration Behaviour of Actinides and Fission Products in the Geosphere, (Migration '91)*, Jerez de la Frontera, Spain, October 21–25, 1991, Abstracts: 77 (1991).

28. R. GUILLAUMONT and J. P. ADOLF, "Behavior of Environmental ^{239}Pu at Very Low Concentrations," *Radiochim. Acta*, **58/59**, 53 (1992).

29. K. L. NASH, J. M. CLEVELAND, and T. F. REES, "Speciation Patterns of Actinides in Natural Waters: A Laboratory Investigation," *J. Environ. Radioac.*, **7**, 131 (1988).

30. H. A. FRIEDMAN and A. D. KELMERS, "Laboratory Measurement of Radionuclide Sorption in Solid Waste Storage Area 6 Soil/Groundwater Systems," ORNL/TM-10561, Oak Ridge National Laboratory (1990).

Robert A. Fjeld (BS, nuclear engineering, North Carolina State University, 1970; MS, 1972, and PhD, 1976, nuclear engineering, The Pennsylvania State University) is the Dempsey Professor of environmental engineering and science at Clemson University. He teaches and conducts research in the environmental aspects of nuclear technologies including radionuclide transport, radioactive waste management, and risk assessment.

Timothy A. DeVol (BS, engineering physics, Ohio State University, 1987; MS, 1988, and PhD, 1993, nuclear engineering, University of Michigan) is an assistant professor of environmental engineering and science. He teaches and conducts research in the areas of environmental radiation measurements, environmental health physics, and radioactive waste management.

Russell W. Goff (BS, chemistry, Emory University, 1989; MS, environmental systems engineering, Clemson University, 1994) is a project manager at URS Corporation in Oak Ridge, Tennessee. He is responsible for managing staff and marketing new information technologies as related to hazardous waste remediation and environmental compliance.

Matthew D. Blevins (BS, chemistry, West Virginia University, 1993; MS, environmental systems engineering, Clemson University, 1995) is a project manager at the Nuclear Regulatory Commission in Washington, D.C. He performs environmental reviews and manages the preparation of environmental impact statements.

David D. Brown (BS, physics, Muhlenberg College, 1990; MS, environmental systems engineering, Clemson University, 1995) is a health physicist at the Nuclear Regulatory Commission in Washington, D.C. He is the lead reviewer in the areas of both health physics and environmental protection for a licensee's application for a uranium-plutonium mixed-oxide fuel fabrication facility.

Steven M. Ince (BS, chemical engineering, University of Tennessee, 1992; MS, environmental systems engineering, Clemson University, 1996) is a financial analyst for Babcock and Brown in San Francisco, California.

Alan W. Elzerman (BA, chemistry, Williams College, 1971; PhD, water chemistry, University of Wisconsin–Madison, 1976) is a professor and chair of Environmental Science and Engineering at Clemson University. In addition to his administrative duties as department chair, he teaches and conducts research in environmental chemistry and in the sources, fate, analysis, and control of chemicals in natural and engineered environmental systems.

Meredith E. Newman (BS, biology, Southern College, 1981; MS, 1985, and PhD, 1990, environmental systems engineering, Clemson University) is an assistant professor of chemistry at Hartwick College. From 1992 to 1996 she was a senior scientist in the Integrated Earth Sciences Division at the Idaho National Engineering and Environmental Laboratory. Her current teaching and research interests are in the fate and transport of chemicals in the environment and in hazardous waste remediation and treatment processes.